Linear and nonlinear state-space controllers for magnetic levitation

Article *in* International Journal of Systems Science · November 1996

DOI: 10.1080/00207729608929322

2 authors:

Walter Barie
Benshaw
1 PUBLICATION **166** CITATIONS
SEE PROFILE

John Chiasson
Boise State University
147 PUBLICATIONS **8,354** CITATIONS
SEE PROFILE

International Journal of *Systems Science, 1996,* volume 27, number 11, pages 1153-l 163

Linear and nonlinear state-space controllers for magnetic levitation

WALTER BARIE† and **JOHN** CHIASSON†

The problem of precisely controlling (within sensor resolution) the height of a steel ball ahoae the ground by levitating it *against the force of gravity using an electromagnet is considered. The state variables used to model the system are the hall's position below the magnet, the ball's speed and the current in the electromagnet. Two state-space controllers are compared in terms of their performance in controlling the hall's position. The first controller is based on feedback linearization where a nonlinear state-space transformation along with nonlinear state feedback is used to linearize the system exactly. A linear controller is then used* on *the resulting* system *to control the ball's position. As a direct measurement of ball speed is* not *available, a nonlinear observer with linear error dynamics is used to estimate the speed. The second controller is a standard linear state feedback controller whose design is based* on *a linear model found by perturbing the nonlinear system model about an operating point. A linear observer is used to estimate the ball's velocity. Experimental results are presented to compare the effectiveness of the two controllers in terms of their ability to respond to step inputs and to track sinusoidal reference trajectories.*

1. Introduction

Magnetic levitation systems have many varied uses such as in frictionless bearings, high-speed maglev passenger trains, levitation of wind tunnel models, vibration isolation of sensitive machinery, levitation of molten metal in induction furnaces and the levitation of metal slabs during manufacture (Laithwaite 1965, Jayawant and Rea 1965). These systems have nonlinear dynamics that are open-loop unstable and, as a result, feedback control is required to stabilize them. The controllers for these systems were designed using standard linear control techniques, i.e. based on an approximate linear model found by perturbing the system dynamics about a desired operating point. As this linear model of the system is valid only about a 'small' area of the operating point, the resulting linear controller can only be expected to function well in this same region. This approach to nonlinear control design is widely used since it is relatively straightforward to design a linear controller to stabilize the linear model and thus, the nonlinear system in a neighbourhood of the operating point. However, this methodology does have drawbacks. For example, if a disturbance acts on the system so that it strays (relatively) far from the operating point, it can go unstable. Also, linear controllers typically require some kind of gain scheduling procedure to change operating points.

Our interest here is the study of nonlinear versus linear state-space techniques for the control of the position (height) of a steel ball levitated above the ground by an electromagnet (Figs 1 and 2). A linear controller for such a system was designed and implemented by Wong (1986). There, the nonlinear system equations were perturbed about an operating point, resulting in an approximate linear model which has a pole in the open right-half plane. Wong was able to show that a (linear) phase-lead compensator was sufficient to stabilize the system for step responses of 1·5 mm about the operating point. The parameters of the phase-lead controller were chosen using root locus techniques and the controller was implemented using discrete analogue electronic components. Cho *et al.* (1993) did a comparison of a sliding mode controller versus a linear phase-lead controller. For that study, the sliding mode controller was shown to provide a better transient response than the linear controller. Cho et *al.*

Received 10 January 1996. Accepted 18 April 1996.

† This work was done while the authors were affiliated with the Department of Electrical Engineering at the University of Pittsburgh. The authors are now employees of ABB Dailmer-Benz Transportation, 1501 Lebanon Church Road. Pittsburgh. PA 15236-1491, U.S.A.e-mail: john.n.chiasson@USAEG.mail.abb.com.

0020-7721/96 $12.00

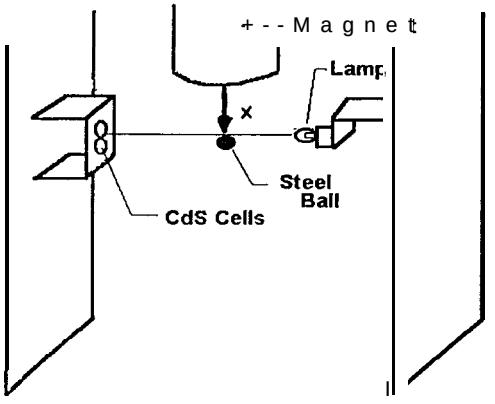

Figure 1. Schematic of magnetic levitation system.

(1993) neglected the current dynamics in their model and did not use current in their feedback controller. Further, the position sensor constructed in the experimental set-up of Cho et al. (1993) was limited to a range of 1 mm and, consequently, the ball's motion was limited to this range.

In the work presented here, a nonlinear controller is used in conjunction with a nonlinear velocity observer to provide tracking/regulation of the levitation height of a steel ball. Specifically, the state-space model consisting of ball position, ball speed, and magnet current is feedback linearizable and it is also possible to construct a nonlinear observer with linear error dynamics to estimate the ball's velocity from measurements of position and current. Based on these methods, a state feedback controller and observer are designed and implemented to control the height of a levitated ball. For comparison, a linear state feedback controller and observer (based on a linear system model) are also implemented.

The experiments show that the two controllers are comparable in their responses to step inputs. However, it is shown that the feedback linearization controller can provide significantly better trajectory tracking (i.e. smaller tracking error and tracking of more demanding trajectories) compared with the linear controller. In particular, the nonlinear controller allows the ball to track sinusoidal reference trajectories whose frequencies are beyond the bandwidth R/L of the electromagnet.

2. Mathematical model

Figure 1 is a diagram of the levitation system while Fig. 2 is a photograph of the actual system. Note that the ball position x is positive increasing in the downward direction.

The dynamic equations of the magnetic levitation system are (Wong 1986, Cho *et* al. 1993, Woodson and Melcher 1968)

$$\left.\begin{aligned} \frac{dx}{dt} &= v \\ Ri + \frac{d(L(x)i)}{dt} &= e \\ m\frac{dv}{dt} &= mg - C(i/x)^2, \end{aligned}\right\} \qquad (1)$$

where x denotes the ball's position, v is the ball's velocity, i is the current in the coil of the electromagnet, e is the applied voltage, R is the coil's resitance, L is the coil's inductance, g is the gravitational constant, C is the magnetic force constant and m is the mass of the ball. As indicated in (l), the inductance $L(x)$ is a nonlinear

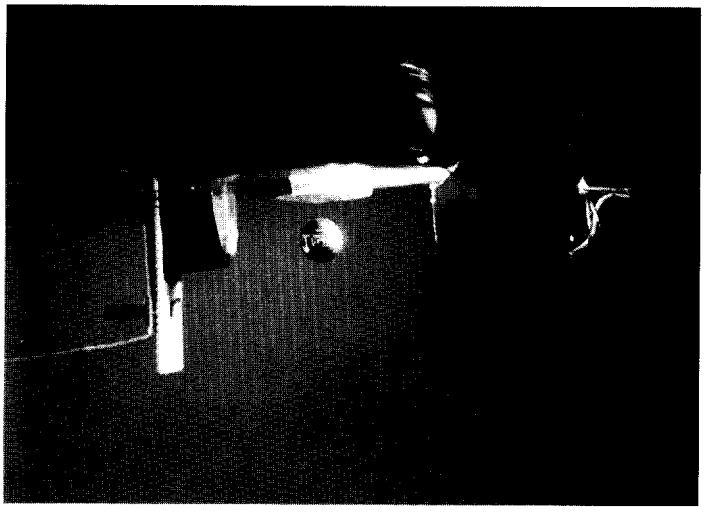

Figure 2. Photograph of magnetic levitation system.

function of the ball's position x (Wong 1986, Woodson and Melcher 1968). A typical approximation is to assume that this inductance varies inversely with respect to the ball's position x (Wong 1986), that is

$$L(x) = L_1 + L_0 x_0/x, \tag{2}$$

where x_0 is an arbitrary reference position for the inductance. Another approximation for $L(x)$ is given by Woodson and Melcher (1968)

$$\mathrm{L(x)} = L_1 + L_0/(1 + x/a). \tag{3}$$

However, over the range of x considered in the experiments, one can pick the parameters L_0, L_1 and a in (3) so that it closely approximates (2). Therefore, because of its simplicity, the approximation (2) was used. Substituting (2) into the second equation of (1) results in

$$e = Ri + L\,\mathrm{d}i/\mathrm{d}t - (L_0 x_0 i/x^2)\,\mathrm{d}x/\mathrm{d}t. \tag{4}$$

A conservation of energy argument shows that $\mathrm{C} = L_0 x_0/2$ (Barie 1994). Combining the above with $x_1 = x$, $x_2 = \mathrm{v}$, $x_3 = i$ and $u = \mathrm{e}$, the system equations in state-space form are

$$\left.\begin{aligned} \mathrm{d}x_1/\mathrm{d}t &= x_2 \\ \mathrm{d}x_2/\mathrm{d}t &= g - \frac{C}{m}(x_3/x_1)^2 \\ \mathrm{d}x_3/\mathrm{d}t &= -\frac{R}{L}x_3 + \frac{2C}{L}(x_2 x_3/x_1^2) + \frac{u}{L}. \end{aligned}\right\} \tag{5}$$

3. Exact linearization controller

Consider the nonlinear change of coordinates (Chiasson 1989)

$$\left.\begin{aligned} z_1 &= \mathrm{T,(x)} = x_1 \\ z_2 &= \mathrm{T^*(x)} = x_2 \\ z_3 &= T_3(x) = g - (C/m)(x_3/x_1)^2. \end{aligned}\right\} \tag{6}$$

This is a feedback linearizing transformation (Nijmeijer and der Schaft 1990, Isidori 1989). The system state is restricted to the region of the state-space where $x_1 > 0$ and $x_3 > 0$ to ensure the transformation (6) is invertible. Note that the transformation (6) results in the **new** state variables z_1, z_2, z_3 being the ball's position, velocity, and acceleration, respectively.

In these new coordinates, the system equations become

$$\left.\begin{aligned} \dot{z}_1 &= z_2 \\ \dot{z}_2 &= z_3 \\ \dot{z}_3 &= r(x) + \beta(x)u, \end{aligned}\right\} \tag{7}$$

where

$$\alpha(x) = \frac{2C}{m}\left(\left(1 - 2\frac{C}{L}\right)\frac{x_3^2 x_2}{x_1^3} + \frac{R}{L}\frac{x_3^2}{x_1^2}\right)$$

$$\beta(x) = -2Cx_3/Lmx_1^2.$$

Using the state feedback

$$u = (-\alpha(x) + w)/\beta(x) \tag{8}$$

results in the linear state-space representation

$$\begin{bmatrix} \dot{z}_1 \\ \dot{z}_2 \\ \dot{z}_3 \end{bmatrix} = \begin{bmatrix} 0 & 1 & 0 \\ 0 & 0 & 1 \\ 0 & 0 & 0 \end{bmatrix}\begin{bmatrix} z_1 \\ z_2 \\ z_3 \end{bmatrix} + \begin{bmatrix} 0 \\ 0 \\ w \end{bmatrix}. \tag{9}$$

The term $\beta(x)$ is zero if and only if $x_3 = i = 0$. In the experiments reported here, the current is kept positive and bounded away from zero so the singularity of $\beta(x)$ is not an issue. Let an arbitrary reference trajectory $(z_{1\mathrm{ref}}(t), z_{2\mathrm{ref}}(t), z_{3\mathrm{ref}}(t))$ and reference input $j_{\mathrm{ref}}(t)$ be given such that $z_{1\mathrm{ref}}(t) = x_{\mathrm{ref}}(t)$, $z_{2\mathrm{ref}}(t) = \mathrm{d}z_{1\mathrm{ref}}(t)/\mathrm{d}t$, $z_{3\mathrm{ref}}(t) = \mathrm{d}z_{2\mathrm{ref}}(t)/\mathrm{d}t$, $j_{\mathrm{ref}}(t) = \mathrm{d}z_{3\mathrm{ref}}(t)/\mathrm{d}t$. A linear feedback for w is then chosen as

$$\begin{aligned} \mathrm{w} = K_0 \int_0^t (z_{1\mathrm{ref}} - z_1)\,\mathrm{d}t + K_1(z_{1\mathrm{ref}} - z_1) \\ + K_2(z_{2\mathrm{ref}} - z_2) + K_3(z_{3\mathrm{ref}} - z_3) + j_{\mathrm{ref}}. \end{aligned} \tag{10}$$

As the system (9) is in control canonical form, it is straightforward to choose the feedback gains K_0, K_1, K_2 and K_3 to place the closed-loop poles of the system in the left-half plane to ensure tracking of the reference trajectory.

3.1. Nonlinear velocity observer with linear error dynamics

The feedback linearization controller requires knowledge of all three state variables. However, only two of the state variables, the ball position and electromagnet coil current are directly measurable. Therefore the ball's velocity must be estimated for use by the feedback controller.

One could estimate the velocity by numerically differentiating the measured position data. As is well-known, this method will amplify any (especially high-frequency) noise in the position measurement. To get around potential noise problems, the differentiated signal could be filtered, but any causal filter will introduce a delay in the estimate which can degrade controller performance. To avoid all of these difficulties, a reduced-order nonlinear velocity observer is used in this

work. Specifically, from (5) we have

$$\left.\begin{aligned}\frac{\mathrm{d}}{\mathrm{d}x}\begin{bmatrix}x_1\\x_2\end{bmatrix}&=\begin{bmatrix}0&1\\0&0\end{bmatrix}\begin{bmatrix}x_1\\x_2\end{bmatrix}+\begin{bmatrix}0\\g-\dfrac{C}{m}\left(\dfrac{x_3}{x_1}\right)^2\end{bmatrix}\\ y_1&=[1\quad 0]\begin{bmatrix}x_1\\x_2\end{bmatrix}.\end{aligned}\right\}\qquad(11)$$

As the electromagnet current x_3 and ball position x_1 are directly measured, a reduced-order observer can then be defined by inspection as

$$\left.\begin{aligned}\frac{\mathrm{d}}{\mathrm{d}t}\begin{bmatrix}\hat{x}_1\\\hat{x}_2\end{bmatrix}&=\begin{bmatrix}0&1\\0&0\end{bmatrix}\begin{bmatrix}\hat{x}_1\\\hat{x}_2\end{bmatrix}+\begin{bmatrix}0\\g-\dfrac{C}{m}\left(\dfrac{x_3}{x_2}\right)^2\end{bmatrix}\\&\quad+\begin{bmatrix}l_1\\l_2\end{bmatrix}(y_1-\hat{y}_1)\\ \hat{y}_1&=[1\ 0]\begin{bmatrix}\hat{x}_1\\\hat{x}_2\end{bmatrix}.\end{aligned}\right\}\qquad(12)$$

Subtracting (I 2) from (11) gives the error dynamics of the observer, that is, with

$$A_0=\begin{bmatrix}0&1\\0&0\end{bmatrix},\quad c_0=[1\quad 0]$$

$$l=\begin{bmatrix}l_1\\l_2\end{bmatrix},\qquad e=\begin{bmatrix}x_1-\hat{x}_1\\x_2-\hat{x}_2\end{bmatrix},$$

the error dynamics are described by the linear system

$$\dot{e}=(\mathrm{A},-lc_0)e.\qquad(13)$$

As the pair $\{c_0, \mathrm{A},)$ is observable, 1 is used to place the poles of A, $-lc_0$ appropriately in the left-half plane. In this work, the observer poles were placed so that the observer dynamics were much faster (at least five-times) than the dominant poles of the system. Note that the original system (11) is nonlinear in x_1 and x_3. However, as these state variables are measured, the observer (12) uses them as known inputs with the result that the nonlinear term $\mathrm{g}-(C/m)(x_3/x_1)^2$ cancels out in the error system (13) (Krener and Isidori 1983, Krener and Respondek 1985).

4. Linear controller

The linear (perturbation) approximation to the model *(5)* is given by

$$\delta\dot{x}=\boldsymbol{A}\delta x+\boldsymbol{b}\delta u$$

$$\mathrm{y}=\boldsymbol{c}\delta x$$

where

$$\left.\begin{aligned}\boldsymbol{A}&=\begin{bmatrix}0&1&0\\\dfrac{2Cx_{30}^2}{mx_{10}^3}&0&-\dfrac{2Cx_{30}}{mx_{10}^2}\\0&\dfrac{2Cx_{30}}{Lx_{10}^2}&-\dfrac{\boldsymbol{R}}{\boldsymbol{L}}\end{bmatrix}\\ b&=\begin{bmatrix}0\\0\\\dfrac{1}{L}\end{bmatrix},\quad \boldsymbol{c}=[1\quad 0\quad 0]\end{aligned}\right\}\qquad(14)$$

with $x_{10}=x_0$ and $x_{30}=i_0$ satisfying $my=C(x_{30}^2/x_{10}^2)$. The variation in L with the position x_0 was neglected, as it will be shown below that L_0x_0/x is more than 25 times smaller than L_1.

The equilibrium point is $(x_{10}, x_{20}, x_{30})=(x_0, 0, i_0)$ with reference input $u_0=Rx,=Ri_0$. The state variables are $\delta x_1=\mathrm{x}-x_0$, $\delta x_2=\mathrm{v}$, $\delta x_3=x_3-i_0$ and the input is $\delta u=u-u_0=\mathrm{e}-Ri_0$. The linear observer

$$\mathrm{d}\delta\hat{x}/\mathrm{d}t=\boldsymbol{A}\delta\hat{x}+\boldsymbol{b}\delta u+l(y-\hat{y}),\ 1\in\Re^3$$

$$\hat{y}=\boldsymbol{c}\delta\hat{x}$$

was implemented to obtain the speed estimate $\hat{v}=\delta\hat{x}_2$. The reference trajectory is chosen to be the same as that of the nonlinear controller so that $x_{1\mathrm{ref}}=z_{1\mathrm{ref}}$, $x_{2\mathrm{ref}}=z_{2\mathrm{ref}}$ and $x_{3\mathrm{ref}}=i_{\mathrm{ref}}=(x_{30}/2g)(-z_{3\mathrm{ref}}+(x_{30}/x_{10})z_{1\mathrm{ref}})$. The feedback, written in terms of the unperturbed state variables, is then

$$u=K_0\int_0^t(x_{1\mathrm{ref}}-x_1)\,\mathrm{d}t+K_1(x_{1\mathrm{ref}}-x_1)+K_2(x_{2\mathrm{ref}}-x_2)+K_3(x_{3\mathrm{ref}}-x_3)+u_{\mathrm{ref}},\qquad(15)$$

where

$$u_{\mathrm{ref}}=Rx_{3\mathrm{ref}}+\left(\frac{Lx_{30}}{x_{10}}-\frac{2mg}{x_{30}}\right)x_{2\mathrm{ref}}-\left(\frac{Lx_{30}}{2g}\right)j_{\mathrm{ref}}$$

5. Experimental apparatus

The magnetic levitation system consists of a steel ball of mass 11.87 g and radius 7.14 mm, an electromagnet, a Motorola DSP56001 microprocessor development system, an Aerotech 4020 linear amplifier, an interface board with an 8-bit A/D for the current measurement and a 12-bit D/A for the voltage input, a Motorola $\sigma-$ A 16 bit A/D converter for the position measurement and two light sensitive resistors for the position sensitive resistors for the position sensor.

In Wong (1986), Cho *et al.* (1993) and Woodson and Melcher (1968), position sensors were implemented by shining either a visible or infrared light across the arch of the apparatus (right to left in Figs 1 and 2 and measuring the voltage from a light sensitive resistor located at the other side of the arch. Cho *et al.* (1993) used an infrared LED with a photo-transistor detector while Wong (1986) employed a white light source with a CdS light sensitive resistor for detection of the position. A system similar to Wong (1986) was used in our work. Specifically, incandescent light along with two CdS light-sensitive resistors (one directly above the other) were used to obtain a sensor range of approximately 5·2 mm.

The current was sensed by measuring the voltage across a precision 0·1 Ω resistor in series with the electromagnet's coil. The A/D has 8-bits to cover the ± 1.56 A range of current resulting in a quantization error of 12.5 mA.

The electromagnet was constructed similar to the one used by Wong (1986). The magnet consists of 3600 turns of #20·5 AWG wire around a mild steel core with a DC resistance of R = 27.7 Ω (room temperature) and R = 29.7 Ω (warm). The inductance L_1 of the electromagnet (see (2)) was measured and found to be 0·65 Henry.

The controller/observer algorithms were implemented using a Motorola DSP56001 fixed-point microprocessor operating at a clock speed of 20.48 MHz. Both the nonlinear and linear controllers were written in assembly language for execution of the DSP56001 system. The controller is interrupt driven at a sample rate of 1250 Hz. The maximum sample rate is limited to 1250 Hz due to the constraint that the microprocessor must complete the controller calculations and command the appropriate output before the next interrupt occurs.

5.1. Position sensor calibration

The position sensor was calibrated using a precision vertical positioning table with a resolution of 0·02 mm. This was carried out as follows. The steel ball was attached to the top of the positioning table with the table then placed below the magnet. Next, the table was moved up until the ball touched the bottom of the magnet with this position taken as the zero point. The table was then lowered in steps of 0·158 75 mm with the A/D channel of the CdS light-sensitive resistor sampled at each step. This method of calibrating the sensor gives the position with respect to the top of the ball. As the position x_1 in (5) is with respect to the centre of mass of the ball, the radius of the ball is added to the sensor reading to get x_1. The data curve used to calibrate the ball position with the sensor's A/D reading is given by Barie (1994).

In order to avoid the use of a look-up table in the controller program, a third-order polynomial fit was found for the data. The resulting conversion expression from the DSP voltage reading of the sigma-delta A/D to the corresponding position x is given by

$$x = -0{\cdot}873(\mathrm{DSP_{in}})^3 + 1{\cdot}097(\mathrm{DSP_{in}})^2 + 5{\cdot}3066(\mathrm{DSP_{in}}) + 15.049 \text{ (mm)}.$$

The fit of this curve to the measured data has a zero mean error with a standard deviation of σ = 0·045 mm.

5.2. Determination of the force constant

The magnetic force is given by (1) where C is an unknown constant parameter. To determine C, an approach similar to that of Cho *et al.* (1993) was used. Specifically, the ball is placed on a non-magnetic stand directly under the electromagnet. The ball's exact position is recorded by the calibrated position sensor. Next, a slowly rising ramp voltage is applied to the electromagnet and the resulting ball position and electromagnet current is measured. At the first instant of movement (i.e. where the magnetic force equals the gravitational force), the ball's position and the coil's current are recorded. The force constant is then given by $C = mg/(i^2/x^2)$ upon substituting in the measured values for position and current. This procedure was carried out 15 different times varying x over the range of the position sensor. The value for C was taken to be the average of these estimates which turned out to be $C_{\mathrm{ave}} = 1.16 \times 10^{-4}$ Nm^2 A^2. Using this initial value of C, the system could be stabilized so that position and current data of some sinusoidal responses could be measured. Using the measured ball position and electromagnet current data from the sinusoidal trials, a least-squares identification was performed offline to identify C more accurately. The least-squares identified C was found to be C = 1.24×10^{-4} Nm^2 A^2 which is a 6·5% difference.

In order to investigate the validity of the mathematical model of the system, the ball acceleration was reconstructed from the measured ball position data by computing $\mathrm{d}^2x/\mathrm{d}t^2$ and filtering it through a distortionless low-pass filter using the filtfilt command in MATLAB. Denoting the filtered result as $\alpha_{\mathrm{reconst}}$, Fig. 3 is a comparison of it with the ball acceleration calculated from the mathematical model (1), i.e. $g - (C/m)(i/x)^2$. The closeness of the two indicates the validity of the model (1).

Note that L_0x_0 = 2C was used in (2). In the experiments the position x is greater than 10 mm so that $L_0x_0/x \leq 2.48 \times 10^{-2}$ while L_1 = 0·65 making it more than 25 times smaller than L_1.

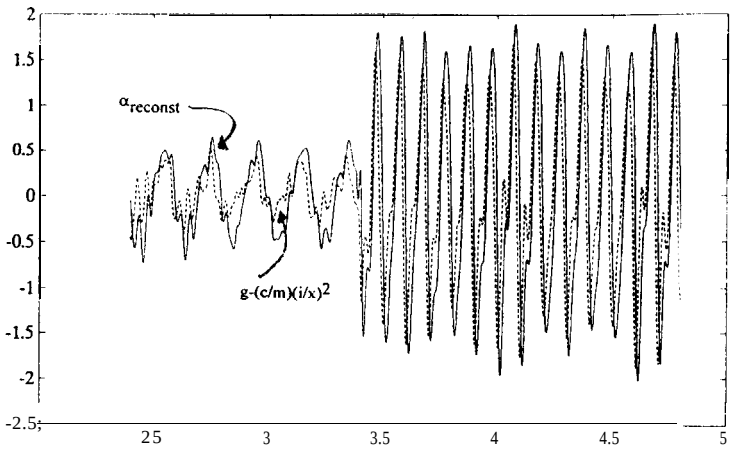

Figure 3. $\alpha_{reconst}$ and $g-(c/m)(i/x)^2$ in millimetres per second per second versus time in seconds.

6. Experimental results and discussion

Experiments were performed to compare the performance capabilities of the nonlinear and linear state feedback controllers. Their performance was compared in terms of their response to step inputs and their ability to provide tracking of sinusoidal reference trajectories.

6.1. *Step responses*

The first experiment consisted of a 4·5 mm step response. As Fig. 4 shows, the ball is lifted off its stand to an initial levitated height of 18·5 mm for the nonlinear control experiment and 18.4 mm for the linear control experiment. The feedback/observer gains were set as K" = 2 x 10^6, K, = 950000, K_2 = *80000*, K_3 = *900*, l_1 = 2000, l_2 = 1 x 10^6 for the nonlinear controller resulting in the feedback linearized system's closedloop poles being — 2.7, — 10.9, — 84.7, — 801 and the poles of the observer error system being at — 1000, — 1000. The gains for the linear controller were set at K_0 = — *58 564*, K_1 = — *53 478*, K_2 = *-2536*, K_3 = *856*, l_1 = 1.6188, l_2 = 982, l_3 = -5869.9 putting the system's closed-loop poles at — 3.43, — 7.42, — 128, — 1207 and the poles of the observer's error system at — 1000, — 1000, — 1000. The feedback gains were manually tuned to reduce the position variations (jitter) about the desired ball position as much as possible without compromising rise-time or dampening of the step response. In this regard, choosing the gains to place the poles any further in the left-half plane (to decrease rise-time further) resulted in amplifier saturation.

A 4·5 mm upward step is introduced into the system at t = 1 s by changing the ball's reference position. The velocity and acceleration references were set to zero. Figure 4 shows that the ball is moved under control to its final position of 14 mm below the electromagnet with the two controllers being comparable in terms of performance. The average steady-state tracking error for both controllers is shown in Fig. 5 and is zero.

However, there is approximately ± 0·04 mm of position

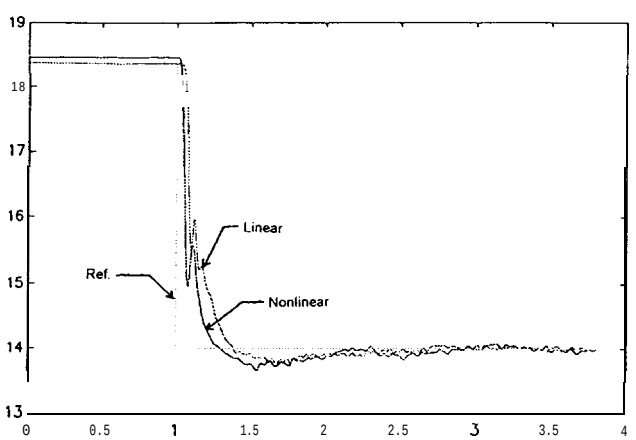

Figure 4. Position step responses in millimetres versus time in seconds.

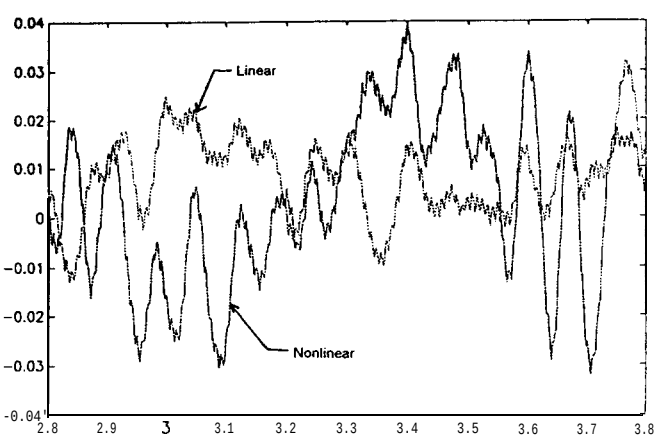

Figure 5. Position error in millimetres due to quantization noise versus time in seconds.

variation about the desired ball position using the nonlinear controller and approximately $\pm 0{\cdot}03$ mm of variation using the linear controller, that is, the linear controller actually gives a slightly smaller steady-state variation about the desired position (note that we were able to put the poles of the linear system further in the left-half plane compared to those of the nonlinear system). It turns out that this variation (jitter) in position about the desired final position is due to the quantization noise of the A/D. Figure 6 is a plot of the measured current using an 8-bit A/D where the relatively coarse resolution is quite evident. To investigate the effect of this on the controllers, simulations were carried out using the software package SIMNON (Elmqvist *et al.* 1990). Figure 7 is a simulation of the nonlinear control law resulting in position variations of about $\pm 0{\cdot}01$ mm when an 8-bit current A/D is simulated, but a much smaller f0.001 mm position variation when a 12-bit A/D is simulated. Simulations were also completed using the linear control law and the results show that the linear controller is much less sensitive to quantization error in the A/Ds than the nonlinear controller. Specifically, for the linear controller, the steady-state position variations due to the A/D quantization error for either the 8-bit or 12-bit A/D is less than $\pm 0{\cdot}001$ mm (note that 12-bit A/Ds were used by Wong 1986, Cho *et al.* 1993). The sensitivity of the nonlinear control law to the A/D quantization error is expected as the nonlinear control law given by (8) and (10) uses the current measurement $i = x_3$ in four different computations while the linear control law (15) uses it only once. In fact, further investigation showed that the term $K_3(z_{3\text{ref}} - z_3)/\beta(i, x_1)$ in u (see (8) and (10)) was by far the most significant cause of the jitter in position using the nonlinear controller. By removing the quantization effect of the current only in the calculation of the acceleration $z_3 = g - (C/m)(i^2/x_1^2)$ it was found that the jitter in position was reduced to less than 0.001 mm as in the case of the linear control law.

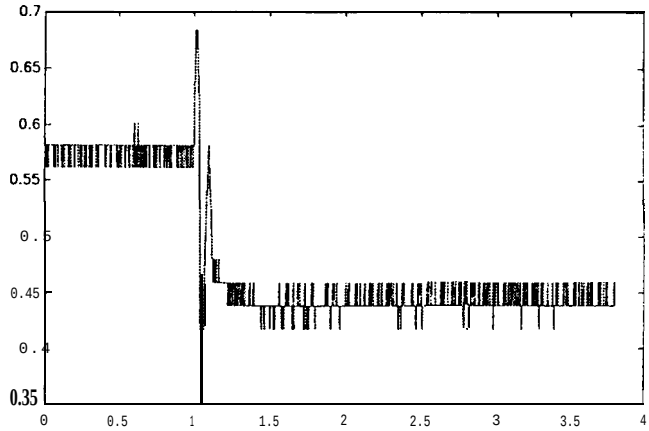

Figure 6. Measured current using an 8-bit A/D in amps versus time in seconds.

Although not presented, in steady-state the nonlinear speed observer's estimated speed stays within ± 1 mm s^{-1} of the reference speed (= 0 mm s^{-1}) while the linear observer was within ± 6 mm s^{-1}. The linear controller also performed satisfactorily using a speed estimate based on backward differentiation (no filtering) in which the steady-state position error was again $\pm 0{\cdot}03$ mm.

6.2. Response to sinusoidal inputs

A sinusoidal trajectory was chosen to test the controllers' trajectory tracking capability. The reference trajectory was chosen as $z_{1\text{ref}} = A \sin(2\pi ft)$, $z_{2\text{ref}} = dz_{1\text{ref}}/dt$, $z_{3\text{ref}} = dz_{2\text{ref}}/dt$ with a corresponding reference input $j_{\text{ref}} = dz_{3\text{ref}}/dt$ where f is the frequency in Hz. Two frequencies were considered: $f = 5$ Hz with A = $0{\cdot}5$ mm and $f = 10$ Hz with A = $0{\cdot}3$ mm. The time constant of the coil is $\tau = L/R = 0.023$ s for a bandwidth (3 dB point) of $1/\tau = 43.2$ rad s^{-1} or $6{\cdot}9$ Hz.

In the first trial, tracking of a 5 Hz sinusoidal

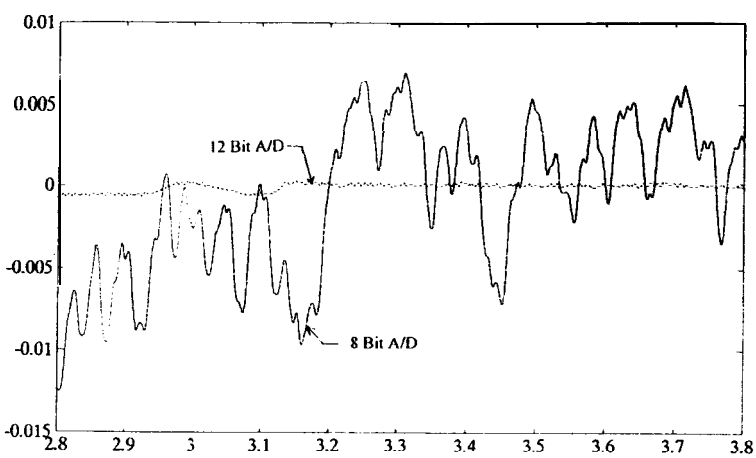

Figure 7. Simulation of the effect of the quantization noise. Ball position in millimetres versus time in seconds.

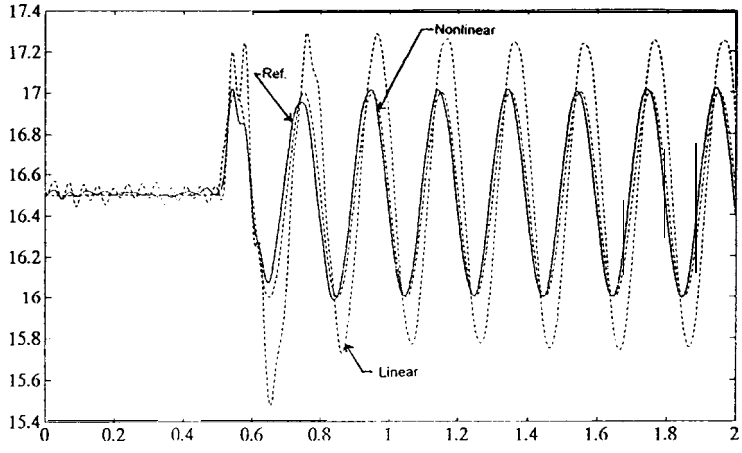

Figure 8. Position response in millimetres versus time in seconds for a 5 Hz sinusoidal reference.

trajectory with a 1 mm peak-to-peak (p-p) amplitude is evaluated. The 5 Hz frequency of the sinusoid was chosen as a frequency below the 3 dB point of the electromagnet. The 1 mm p-p amplitude was chosen to be as large as possible without driving the amplifier into saturation (>40 V). The feedback gains were chosen as K_0 = 6 x 10', $K_1 = 3 \times 10^6$, K_2 = 195000, K_3 = 1050, l_1 = 2000, I, = 1 x 10^6 for the nonlinear controller putting the feedback linearized system's closed-loop poles at $-7{\cdot}4 \pm j16$, — 220, — 8 15 and the poles of the observer error system at — 1000, — 1000. The gains for the linear controller were set at K_0 = -250 000, K_1 = — 95 000, K_2 = -4000 and K_3 = *900*, l_1 = 1.6188, 1, = 982, l_3 = — 5869.9 resulting in the system's closed-loop poles being — 12.3, -57.4, — 170.8, — 1225 and the poles of the observer error system being — 1000, — 1000, — 1000. As for the step responses, the gains were manually tuned to minimize tracking error and position jitter about the desired trajectory.

The position responses of the system using both the nonlinear and linear control laws are given in Fig. 8. The corresponding position tracking errors are given in Fig. 9 where it is seen that the trajectory tracking error oscillates between $\pm 0{\cdot}1$ mm using the nonlinear control law and $\pm 0{\cdot}4$ mm using the linear control law. That is, there is a significant decrease in tracking error using the nonlinear control law. The linear controller was also implemented using a speed estimate based on backward differentiation (no filtering) where the position tracking error was (oscillating) between $\pm 0{\cdot}45$ mm.

Figure 10 gives the reconstructed velocity responses of the system using the nonlinear and linear control laws along with the velocity reference trajectory. The ball velocity was reconstructed offline by differentiating the position data and then passing the result through a distortionless low-pass filter using the non-causal filter program **filtfilt** in MATLAB.

The ball's estimated velocity using the nonlinear

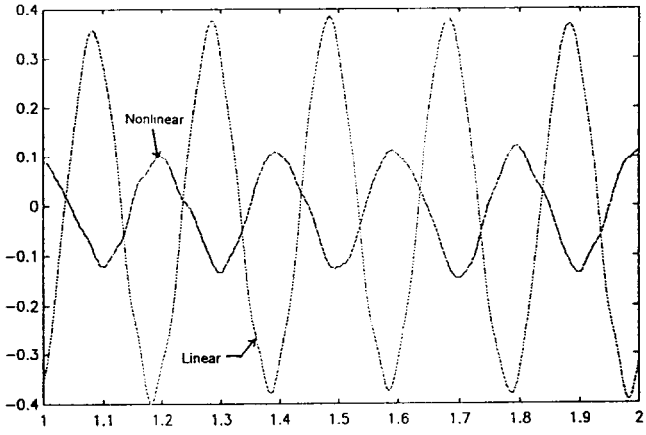

Figure 9. Position tracking error in millimetres versus time in seconds for a 5 Hz position reference.

observer and the reconstructed ball velocity are both given in Fig. 11. The estimation error (error between the observer's estimate and the reconstructed velocity) turned out to be within $\pm$ 6 mm s^{-1}. The estimation error when using the linear observer was larger, being only within ± 15 mm s^{-1}.

Figure 12 is a plot of the reconstructed acceleration response of the system using both the nonlinear and linear control laws along with the reference trajectory. Similar to reconstructing the velocity, the ball's acceleration was reconstructed offline by differentiating the position twice and filtering the result using the non-causal filter **filtfilt** in MATLAB to remove the noise without distorting the signal. It is seen that the ball acceleration does stay with the desired reference trajectory.

In the second trial, tracking of a 10 Hz sinusoidal trajectory with a $0{\cdot}6$ mm peak-to-peak amplitude was calculated. In this case, the 10 Hz frequency of the sinusoid was chosen to be above the open-loop 3 dB point of the electromagnet. The amplitude was reduced

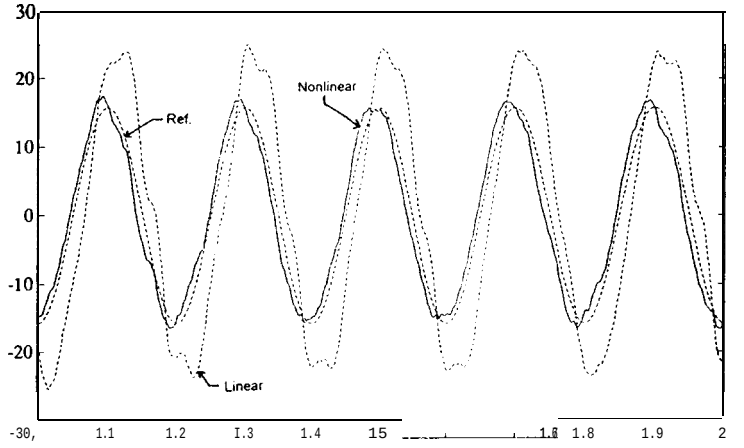

Figure 10. Reconstructed velocity in millimetres per second for a 5 Hz reference.

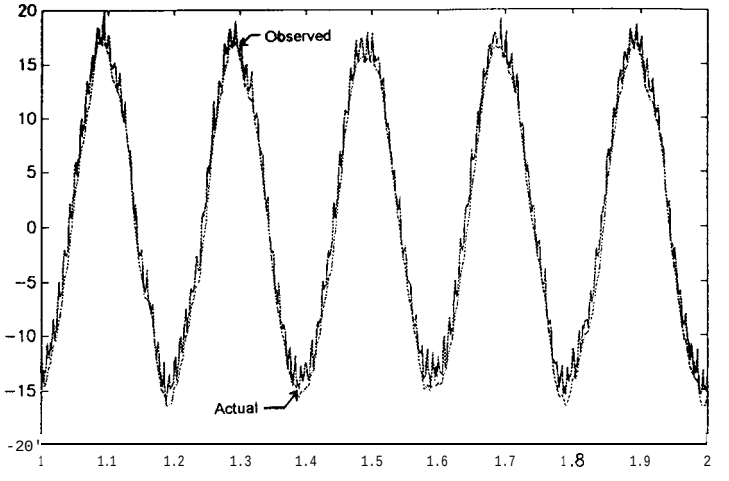

Figure 11. Observer estimated velocity and reconstructed velocity in millimetres per second versus time in seconds for a 5 Hz reference.

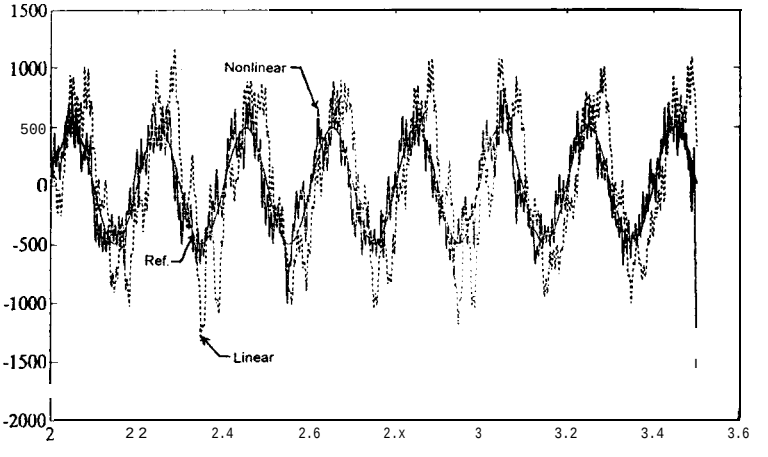

Figure 12. Reconstructed acceleration in millimetres per second per second versus time in seconds for a 5 Hz reference.

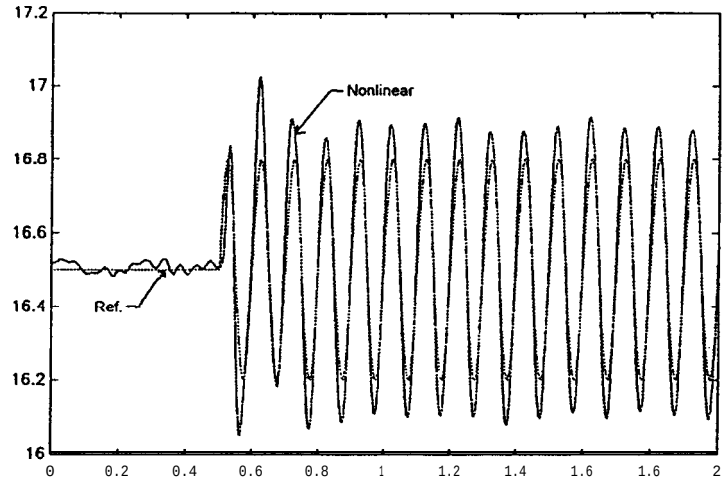

Figure 13. Position responses in millimetres versus time in seconds for a 10 Hz reference trajectory.

to 0·6 mm p-p to prevent amplifier saturation. The feedback gains were the same as in the 5 Hz trial, as manually retuning the gains did not decrease the tracking error. The position tracking response of the system to the 10 Hz trajectory using the nonlinear control law is shown in Fig. 13 where it is seen that the tracking error oscillates between $\pm 0{\cdot}15$ mm. We were unable to achieve any kind of tracking with the linear control law.

The experimental set-up of Cho *et al.* (1993) is different from the one used here and so an exact comparison is not possible. However, some general comments are in order. In Cho et al. (1993), the *R/L* 3 dB point of the electromagnet's coil was 286 rad s^{1} or about 46 Hz, (see equation (25) of Cho et *al.* 1993). They were able to track a 10 Hz position reference signal (well below the 3 dB point of the coil) with a tracking error of about 0·5 mm (Cho et *al.* 1993, Fig. 8) while it was reported that the system went unstable using the linear phase-lead controller. However, neither current measurements nor speed estimates (observer or backward difference) were used by Cho *et al.* (1993) and the current dynamics were taken into account only for the linear controller. In contrast, both the linear and nonlinear controllers presented here were able to achieve tracking of a 5 Hz sinusoidal trajectory (close to the 7 Hz 3 dB point of the electromagnet) by taking into account the current dynamics and employing a state-space trajectory controller feeding back measurements of current, speed (observer or backwards difference) and position.

7. Summary and conclusions

In this paper, a nonlinear controller based on exact feedback linearization theory was compared in terms of tracking performance with a linear state-space controller whose design was based on an approximate linear model of the system. The nonlinear controller turned out to be more sensitive to quantization error in the 8-bit current measurements resulting in slightly larger position variations about the desired position in the step response. However, if a 12-bit A/D was used, simulations showed that the magnitude of the position jitter would equal that of the linear controller. When tracking sinusoidal reference trajectories, the nonlinear controller was found to provide superior tracking performance compared with the linear control law in terms of significantly smaller tracking error and the ability to track higher-frequency trajectories.

Although the set-up in this work was built to study magnetic levitation control of a steel ball, this work is directly relevant to industrial applications. For example, the system (5) is also used to model magnetic bearing systems including those used for the High Accuracy Test Table built by Contraves Inc (Contraves 1993). It is expected that the techniques desribed here would also provide better performance for such systems.

Acknowledgments

The authors wish to thank Dr R. T. Novotnak for his assistance with the Motorola DSP56001 Development System and Professor Joel Falk for providing the precision positioning table used to calibrate the ball's position sensor. A special thanks is due Professor Marc Bodson for his insightful comments on this work. The financial assistance of the Pitt University/Industry Collegium (Aerotech Inc, AEG Transportation Systems, Contraves Inc, General Electric Erie, Robicon Inc) is gratefully acknowledged. The Motorola Corporation is also gratefully achnowledged for donating the DSP56001 Advanced Development System and $\sigma -$ A 16-bit A/D Evaluation Board used in this research.

References

BARIE, W., 1994, Design and implementation of a nonlinear state-space controller for a magnetic Levitation system. M.S. thesis, University of Pittsburgh, Pennsylvania, U.S.A.

CHIASSON, J.. 1989, *EE3648 Nonlinear* Systems Class Notes (Pittsburgh, Pensylvania: University of Pittsburgh).

CHO, D.. KATO, Y., and **SPILMAN,** D. 1993, Experimental comparison of sliding mode and clasical controllers in magnetic levitation systems. *IEEE Control* Systems.

CONTRAVES, 1993, High accuracy test table. *16th Annual Guidance* Test *Symposium,* Holloman AFB, New Mexico, U.S.A.

ELMQVIST, **H.,** ASTRÖM, K., **SCHONTHAL,** T., and **WITTENMARK. B.,** 1990, *SIMNON—User's guide for MS-DOS Computers* (Göteborg, Sweden: SSPA Systems).

ISIDORI, A., 1989, *Nonlinear* Control Systems (New York: Springer-Verlag).

JAYAWANT, B., and **REA,** D., 1965, New electromagnetic suspension and its stabilization. *Proceedings of the Institution of Electrical Engineers,* 115, 5499554.

KRENER, A., and ISIDORI, A., 1983, Linearization by output injection and nonlinear observers, *System and Control Letters, 3, 52-57.*

KRENER, A., and RESPONDEK, W., 1985, Nonlinear observers with linearizable error dynamics, *SIAM Journal on Control and Optimization.*

LAITHWAITE, E., 1965, Electromagnetic levitation. *Proceedings of the Institution of Electrical Engineers,* 112, 2361–2375.

NIJMEIJER, H., and **DER** SCHAFT, A. V., 1990, *Nonlinear Dynamical Control* Systems (New York: Springer-Verlag).

WONG, T., 1986, Design of a magnetic levitation system-an undergraduate project. **IEEE Transactions** *on Education,* **29,** 196–200.

WOODSON, H., and **MELCHER, J.,** *1968, Electromechanical Dynamics—Part 1: Discrete* Systems (New York: Wiley).